

Accounts

Characteristics of Water Adsorbed on TiO₂ Photocatalytic Surfaces as Studied by ¹H NMR Spectroscopy

Atsuko Y. Nosaka* and Yoshio Nosaka*

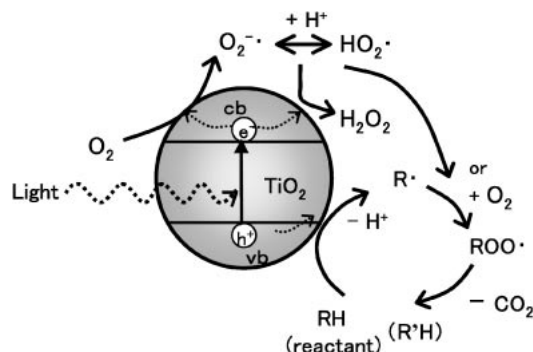
Department of Chemistry, Nagaoka University of Technology, Nagaoka 940-2188

Received February 1, 2005; E-mail: nosaka@nagaokaut.ac.jp

This account is a review of the research on the characteristics of adsorbed water molecules and the photocatalytic reaction sites of incorporated organic molecules on various TiO₂ photocatalysts in powder and film forms by means of ¹H NMR spectroscopy. The adsorbed water can be categorized into four distinctively different water species: i) rigid water species with restricted mobility near the solid surface; ii) less mobile water molecules in the intermediate water layer; iii) relatively mobile water molecules in the outer water layer; iv) very loosely adsorbed water molecules which exchange slowly with gaseous water molecules in air. The temperature dependence of the NMR signal of a small quantity of ethanol molecules incorporated in TiO₂ suggests that the actual photocatalytic reaction site can be these adsorbed water regions. The surface conversion of hydrophilic properties of TiO₂ films induced by photoirradiation is well reflected in the NMR signal change. The enhancement of water molecularly adsorbed on TiO₂ films is evidently detected on UV irradiation; this phenomenon has been difficult to elucidate so far with alternative spectroscopic techniques.

Among the various semiconductor materials, titanium dioxide is one of the most widely studied metal oxides.^{1,2} Since the discovery of photoinduced water splitting on TiO₂ electrodes in 1972,³ a number of studies on photocatalysis by TiO₂ have focused on the enhancement of the photocatalytic efficiency, related to energy renewal and energy storage.^{4–6} However, the recognition of the prominent properties like chemical inertness, photoinduced highly hydrophilic surface, and non-toxicity and high oxidation power for the degradation of hazardous contaminants in air and water, have opened up wider applications of TiO₂ in various fields, such as environmental cleanup, phototherapy, solar cells, antifogging, and self-cleaning of mirrors and glasses.^{7–10}

As illustrated in Scheme 1, irradiation of TiO₂ by UV light



Scheme 1. Reaction mechanism for photocatalytic degradation of organic substrates.

with photon energy higher than its band gap generates excited-state electrons and holes at conduction band and valence band, respectively. These electrons and holes can initiate various redox reactions at the metal oxide surface. In the presence of O₂ and H₂O, the electrons and holes generate various active oxygen species. Organic molecules incorporated into the TiO₂ photocatalytic systems are decomposed through the direct oxidation by the photogenerated holes.¹¹ Thus, TiO₂ has the potential to oxidize a wide range of environmentally hazardous organic contaminants such as dioxins into harmless compounds such as CO₂ and H₂O.

The industrial demand to develop various types of TiO₂ photocatalysts has promoted the research on TiO₂ surface structures at the microscopic level, because the better understanding the physical and chemical properties of the surfaces allows scientists to reveal the relation between surface structure and chemical reactivity. In recent years, one of the most active research subjects is the development of TiO₂ photocatalysts which exhibit enough activity not only under ultraviolet (UV) irradiation but also under visible or solar light irradiation.¹² For this purpose, a number of studies on the characterization of the surfaces of TiO₂ nano-particles and of various TiO₂-based photocatalytic molecular systems have been carried out.¹³

Powders of titanium dioxide characterized by a high specific surface area are prepared using one of two basic methods: combustion of TiCl₄ in the hydrogen/oxygen flame or hydrolysis of titanium sulfate. The different preparation methods of samples results in different crystal defect structures and sur-

face morphologies. Surface defects and surface-adsorbed species have been known to significantly influence the electronic structure and the geometric structure of TiO_2 and in turn to alter its chemical reactivity.¹⁴

In the atmosphere the surface of TiO_2 usually adsorbs water molecules dissociatively to form surface hydroxyls, on which further H_2O molecules are physisorbed through hydrogen bonding. The functions of TiO_2 would be affected by the exertion of the active species produced through the reactions of photogenerated electrons and holes with adsorbed water or hydroxyl groups on TiO_2 . For the better understanding of the various functions of TiO_2 , the properties of adsorbed water have been extensively investigated with a number of spectroscopic techniques.^{15–55}

According to previous work,^{26,42–44} the anatase surface consists predominantly of the most dense (001) plane, with admixtures of (010) and (100) planes having about the same structure. The Ti atoms in these planes are pentacoordinated with respect to oxygen. There are two types of oxygen atoms on each of the (001), (010), and (100) planes of the TiO_2 surface. Oxygen atoms of the first type are coordinated to Ti atoms and have a formal charge $-2/3$, assuming that all the bonds in TiO_2 are purely ionic. They are located 41 pm above the (001) plane. The oxygen atoms of the second type, located 41 pm below the (001) plane, are three-coordinated to Ti atoms and are neutral. For (010) and (100) planes, all oxygen atoms are located in the plane. Dissociation of H_2O molecules over a TiO_2 surface results in the formation of OH groups with the formal charges of $-1/3$ and $1/3$ on the OH protons respectively. The existence of two types of OH groups on the anatase surface was confirmed by IR data with two stretching bands.⁴⁵ The band at 3675 cm^{-1} was attributed to the adjacent OH groups interacting via weak hydrogen bonds, while the band at 3715 cm^{-1} could be attributed to OH groups attached to Ti atoms.

It has been long believed that oxygen defects or Ti^{3+} are required for hydration on TiO_2 surfaces, since the low-defect-density surface is entirely inert toward H_2O adsorption at room temperature, but ion bombardment and generation of Ti^{3+} in an oxygen-deficient lattice creates a surface at which molecular water can adsorb.^{46–48} However, recent experimental results revealed that this is not necessarily the case. Ti^{3+} sites at oxygen vacancies on $\text{TiO}_2(110)$ are active for water dissociation, whereas Ti^{3+} sites on $\text{TiO}_2(100)$ provide no additional reactivity for water dissociation^{23,49–51} and Ti^{3+} sites on Ti_2O_3 surface do not promote water dissociation.^{52–54} Thus since an electronic defect does not necessarily ensure water dissociation, it has been proposed that the geometric arrangement of cations and anions, as well as their general ability to bind water and receive protons, respectively are the key factors in water dissociation activity on an oxide.⁵² Recent STM data revealed that water dissociates at room temperature on $\text{TiO}_2(110)$ step edges, resulting in terminal OH groups at Ti^{4+} step sites.⁵⁵ These OH groups at step sites do not appear to diffuse at room temperature. On the other hand, most of the cation sites on the terraces are unoccupied after water exposure at room temperature.

^1H NMR spectroscopy has been utilized as one of the most effective techniques to investigate water adsorbed on solid

surfaces.^{56–71} The primary advantage of NMR measurements is their quantitative nature. Results often provide information which is unattainable by other spectroscopic techniques. Among the stable nuclei, the proton is the most sensitive nucleus feasible for NMR detection. Therefore, early NMR studies on surfaces were carried out mainly by ^1H NMR spectroscopy. Information on surface OH groups and their interactions with adsorbed molecules has been obtained by the analysis of line shape and relaxation times, which provide information on the geometrical arrangement of the protons and on their motion.^{69–71} However, the technique met with limited success since the large width of the resonance lines due to dipolar interactions between magnetic nuclei made the identification of the individual protons and the measurement of their chemical shifts difficult. The development of NMR spectrometers with high magnetic fields and the line-narrowing techniques made it possible to obtain high resolution NMR spectra of solid catalysts and adsorbed species at very low coverage. Thus, quantitative information on molecular adsorption in catalytic systems and the electronic state of the surface active site became obtainable.

With the use of magic angle spinning (MAS) of the samples to narrow NMR lines, ^1H NMR signals of different surface OH groups bound to certain sites on various catalysts can often be resolved, and an accurate measurement of their chemical shifts becomes possible. Recently, Mastikhin et al. have reviewed the application of ^1H NMR studies of a variety of heterogeneous catalysts.³⁷ They recorded the ^1H MAS NMR spectra of TiO_2 anatase samples obtained from different preparations and dehydrated in vacuum at 523 and 773 K. The high resolution ^1H NMR spectra presented several resonance lines of chemically inequivalent OH groups, depending on the method of preparation and the dehydration temperature. Two main peaks at 6.4 and 2.3 ppm were assigned to the positively charged more acidic protons located on bridged O atoms, and to the more basic H atoms bound to the terminal oxygen, respectively. The other resonance lines were assigned to OH groups bonded to species such as Si, Cl, and S which were contained as impurities in the samples. The acidic OH groups in the hydrated titanium dioxide were reported to be stable in air up to the temperature of 773 K.⁶⁵

Much of the ^1H NMR research on metal oxides focuses on hydroxyl groups or chemisorbed water molecules which adsorb dissociatively on the solid surface after the elimination of physisorbed water molecules because they are closely related to the characteristics of solid surface. However, there have not been many reports so far on the water physisorbed on TiO_2 studied by ^1H NMR.^{63,67} In the practical applications, TiO_2 photocatalysts are used under the aerobic conditions in the presence of physisorbed water. Therefore, it is important as well to characterize these water molecules and to elucidate the role which they play in the actual photocatalytic process for the enhancement of the photocatalytic efficiency on practical usage. To clarify the role of the physisorbed water in the practical photocatalytic reactions, we have been investigating the water molecules adsorbed on the various TiO_2 photocatalysts of different properties by taking advantages of the high sensitivity and quantitative nature of ^1H NMR.

Adsorbed Water on TiO₂ Powders

¹H MAS NMR spectra of anatase abundant TiO₂ powders present a relatively sharp single peak at 295 K, whose line width is several hundreds of Hz at half peak height. The spectra appear to be less informative as compared to those composed of well-resolved resonance lines. There are several conventional strategies to investigate the characteristics of water molecules adsorbed on solid surfaces by ¹H NMR spectroscopy. One of the most popular methods is the measurements of relaxation times, that is, longitudinal relaxation time (*T*₁) and transverse relaxation time (*T*₂).^{68–71} When relaxation times of protons are determined by the inter- and intra-proton–proton dipolar interactions, the relaxation times are described as functions of the interacting proton–proton distances and correlation times,^{72,73} which provide information on the structure and the nature of molecular motions. This strategy is widely exploited in the various fields to determine molecular structures and orientations; a number of researchers are nowadays focusing on the determination of three dimensional structures of large biological molecules such as proteins and nucleic acids not only with ¹H NMR but also with the combination of ¹³C and ¹⁵N NMR^{74,75} using highly sophisticated pulse techniques.⁷⁶ The application of this method to the adsorbed water molecules on photocatalysts is attractive. However, the analysis would not be straightforward because the structures of water molecules would not be unique and the correlation times must be inhomogeneous for heterogeneous systems like TiO₂ photocatalysts.

Another method that is often employed is to detect signal changes at a low temperature below 273 K. This method aims to differentiate the weakly and strongly bonded water molecules in the water/solid interface by lowering the temperature. The strongly bonded water does not freeze at all in the examined temperature range, while the weakly bonded water freezes mostly at a temperature several degrees lower than 273 K. The strongly bonded water molecules are involved in the formation of adsorption complexes with the charged and polar functional groups of the solid surface and are influenced by perturbations from the interface. On the other hand, the weakly bonded water molecules would be localized near the hydrophobic region on the surface.^{66,67,77–79}

From the dependence of the intensity of the ¹H NMR signal of perturbed water molecules on the temperature, Bogillo et al. determined the average thickness of the interface water layer and the total change in water free energy at a water/solid interface in the aqueous and deuteriochloroform suspensions of TiO₂ rutile and this sample modified by sequential coating

with amorphous Al₂O₃ and SiO₂.^{66,67} They deduced that the excess Gibbs energy of water at the water/solid interface and the thickness of the adsorbed water layer increase on the surface modification. The thickness of the water layer perturbed by the modified rutile surface ranges up to 20 nm; the thickness decreases on going from aqueous to deuteriochloroform suspensions. They concluded that the polarization property of the solid particles is responsible for the long-range forces in rutile and its modified form in aqueous suspensions. Thus, they froze bulk water to extract information on the thermodynamic characteristics of adsorbed water. However, with this method it would be difficult to get the information about the physisorbed water weakly adsorbed on the solid surface, since these water molecules are considered to exchange relatively rapidly with bulk water molecules.

Enriquez et al. measured the ¹H NMR spectra of TiO₂ of anatase with different water contents at 100 K.^{63,64} By calculating the shape functions they presented the distribution of the protons between water molecules and surface OH groups and the distances between OH groups. The water molecules equivalent to half of the number of the OH groups are attached to these OH groups by hydrogen bonds. There are two types of OH groups at the surface in equal numbers. One is bound to Ti atoms with a negative charge and another is lattice-bicoordinated to Ti atoms with a positive charge. Each positive OH group is supposed to hydrogen bond a water molecule. On dehydration, water molecules are eliminated and the condensation of OH groups occurs between neighboring groups with opposite charges, resulting in maintaining the charge equilibrium.

Contrary to the low temperature experiments as stated above, we employed different strategies.³⁶ By raising the temperature, we observed the variation of the water signals of TiO₂ powder samples directly under atmospheric conditions and attempted to characterize the physisorbed water by measuring line width, chemical shifts, and peak intensities. This approach is straightforward, and could be successfully applied for the detection of different kinds of water molecules adsorbed on solid metal oxide surfaces. Firstly, we applied this approach to six different commercially available anatase abundant TiO₂ powders, i.e. Degussa P25 (Japan Aerosil), Hombikat UV-100 (Sachtleben Chemie), ST-01 (Ishihara Techno), F4 (Showa Titanium), AMT-100, and AMT-600 (Tayca). The peak area of the proton NMR signals increases corresponding to the surface area of the individual TiO₂ powders.³⁶ The amounts of adsorbed water per unit surface area are almost the same for the six examined photocatalysts, as shown in Table 1, implying that the thickness of the overall adsorbed

Table 1. The Relative Intensities of ¹H NMR Signals and Physical Properties of TiO₂ Photocatalysts^{36,88}

TiO ₂	NMR intensity	Anatase component /%	Primary particle size /nm	BET surface area /m ² g ⁻¹	Peak intensity/surface area
P25	1.0	80	32	49	7.0
F4	1.2	90	28	56	7.3
AMT-600	1.2	100	30	50	8.1
AMT-100	6.3	100	6	260	8.4
ST-01	7.0	100	7	320	7.5
UV-100	8.7	100	10	270	11.0

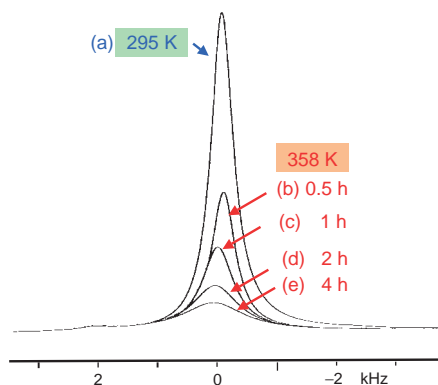


Fig. 1. ^1H MAS NMR spectra of TiO_2 powder (ST-01) measured at 500 MHz with spinning rate of 12.6 kHz at (a) 295 K and (b) 0.5 h, (c) 1 h, (d) 2 h, and (e) 4 h after the temperature was raised to 358 K.³⁶

water layer observed by NMR is almost the same for these six TiO_2 .

The TiO_2 powders are packed into NMR sample tubes in contact with the air through a small hole and the spectral changes have been examined on increase of the temperature up to 358 K under flowing dry air. Figure 1 shows the typical change of the water signal of the examined TiO_2 powders at 358 K. The resonance line becomes broader and shifts slightly with time as volatile water molecules vaporize and are evacuated through the small hole. The intensity gradually decreased to about 30% of the initial value after 4 h. When the temperature is reverted to 295 K, this signal becomes even broader due to the reduced mobility, which is about 3 times that of before the temperature increase. This broad signal is attributed to the highly immobilized water molecules near the solid surface region, which remained in the photocatalytic system after the vaporization of the volatile water molecules. Although before the temperature increase sharp and broad water signals overlap and cannot be distinguished, the rigid water could be detected after the vaporization of the mobile water. The reduced water signal recovers gradually in ambient conditions, as water molecules in the air re-adsorb on the solid surface. The signal intensity recovers almost completely within 20 h for P25, while it takes much longer (about 1 month) for ST-01 whose surface area is about six times larger than that of P25 (Table 1). Thus, the peak which appears to be a single signal turned out to consist of various signals with different line widths and chemical shifts, corresponding to the water molecules of different dynamic structures. These results indicate that the adsorbed water regions are quite complex.

The peak area presents a characteristic time profile at 358 K as shown in Fig. 2; it decreases by 40–50% in the first 10 min, and in the following 2 h decreases further about 20%. The remained 30% of the peak barely changes even after another 2 h. This means that about 50% of the water molecules are very mobile and easy to volatilize, 20% are less mobile and harder to volatilize, and the rest (about 30%) are highly stabilized water molecules. The highly stabilized water signals disappear after the thermal treatment of the sample at 423 K, as shown in Fig. 3, indicating that the observed water signals can be ascribed to the physisorbed water molecules but not to titanol, be-

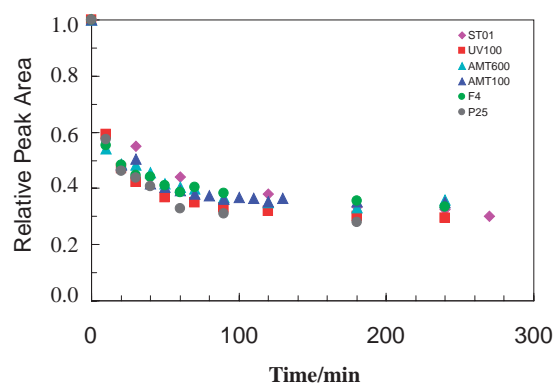


Fig. 2. (A) Time profiles of the relative peak area (the ratio of peak area to that measured at 295 K) of ^1H NMR signals of TiO_2 powders measured at 358 K. (■: UV-100, ◆: ST-01, ▲: AMT-100, ▲: AMT-600, ●: F4, and ●: P25).

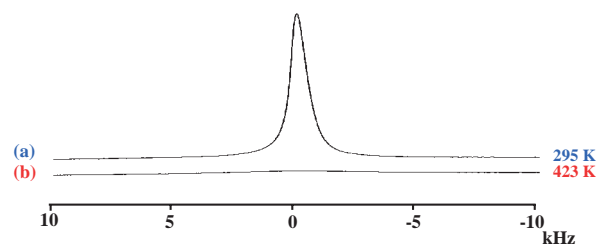


Fig. 3. ^1H MAS NMR spectra of TiO_2 powder (ST-01) measured at 500 MHz with spinning rate of 12.6 kHz at (a) 295 K before calcinations, (b) after calcinations at 423 K for 2 h. NMR measurements were performed just after the calcinations.

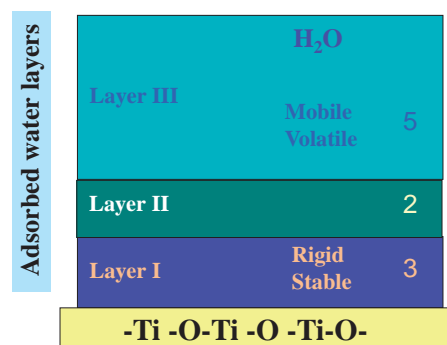


Fig. 4. Plausible structure of water layers I, II, and III at the idealized TiO_2 surface deduced from the ^1H NMR observations.

cause chemisorbed water molecules (titanol) are not eliminated at this temperature.¹⁴ The NMR observations are well consistent with the results of the thermogravimetry measurements for P25 and UV100, in which the decrease of weight at 358 K is about 50 to 70% of that at 423 K, when temperature is raised 10 degree per minutes.⁸⁰ Thus, the water region consists of three distinctly different water species represented by three layers, as illustrated in Fig. 4; (I) the layer with highly immobilized water near the solid surface, (II) the intermediate layer consisting of relatively mobile water, and (III) the outermost

layer with the most mobile (volatile) water. The ratio of the water content in each layer would be 3(I):2(II):5(III). This three layer model would be supported by the observations by temperature-programmed desorption (TPD) spectra measured after adsorbing water molecules on TiO₂ powders of anatase at 140 K under ultrahigh vacuum conditions.²⁷ The spectra presented water desorptions at about 200 and 300 K. Two H₂O peaks at 200 K were assigned to desorption from islands of molecular H₂O. One peak was nonsaturating and assigned to multilayers, whereas another peak appeared as the higher-temperature shoulder was assigned to the monolayer. These two peaks might correspond to the water species in layers III and II observed by ¹H NMR. The TPD peak at 300 K was interpreted as water molecules bound to the surface through hydrogen bonds to surface oxygen anions, which might correspond to the water species in layer I observed by ¹H NMR. The time profiles of peak areas per unit surface area at 358 K for six photocatalysts agreed with each other and are well correlated with those of relative intensities, ensuring also that the thickness of the three layers does not differ significantly among the six photocatalysts.³⁶

From the weight difference of the TiO₂ powder sample before the temperature increase and after the sample was kept at 358 K for 4 h, the number of water molecules could be roughly estimated to be 4.8×10^{14} , 3.2×10^{14} , and 8.0×10^{14} molecules/cm² for layers I, II, and III, respectively. Finnei *et al.* estimated the concentration of H₂O coordinated to the surface of a pre-dried TiO₂ film of anatase to be 5×10^{14} molecules/cm², which corresponds to an initial coordination of H₂O species to 65% of the available Ti⁴⁺ sites at the preferentially exposed anatase (101) surface. The concentration decreased to 0.65×10^{14} molecules/cm² over the temperature range from 300 to 423 K.⁴¹ On the other hand, for the TiO₂ of rutile, on the basis of the TPD observation, Henderson estimated the exposure at which the first layer saturated on the (1 × 1) surface of the (100) facet to be about 7.5×10^{14} molecules/cm².³² Because this exposure is approximately equivalent to the surface number density of five coordinate Ti⁴⁺ sites on the (1 × 1) surface (7.36×10^{14} molecules/cm²), he suggested that water molecules in the first layer bind these sites.

The line widths of ¹H NMR signal of TiO₂ become broader with time at 358 K, as the less-mobile broader water signals successively appear; these widths show notable differences among the six photocatalysts. These results suggest that the nature of the molecular motion and structures of water molecules are different in the inner layers, particularly in layer I. The line widths become broader in the order of ST-01 < UV-100 < P25 < AMT-100, AMT-600, and F4. Provided that the line width (spin-spin relaxation rate) is determined predominantly by dipole-dipole interactions between protons, the water molecules in layer I for ST-01, UV-100, and P25 would be in more mobile states as compared to those for the other three TiO₂. Water molecules interact with ionic surfaces by various types of forces and are capable of self-association and organization of long-range order on solid surfaces. The molecular motions of water in adsorbed layers and the degree of dissociation likewise depend on the nature of the underlying surface.

The time profiles of chemical shifts measured at 358 K for

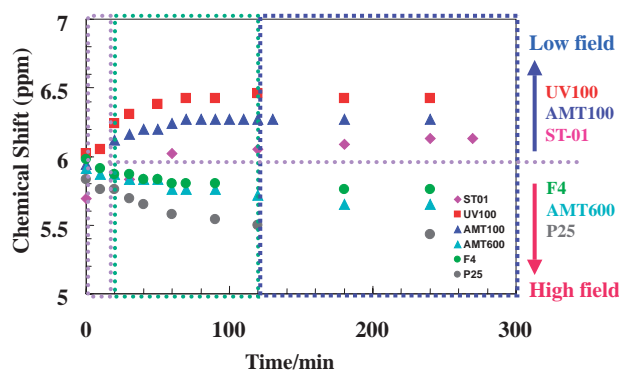


Fig. 5. Time profiles of chemical shifts of ¹H NMR signals of TiO₂ powders measured at 358 K. (■: UV-100, ◆: ST-01, ▲: AMT-100, ▲: AMT-600, ●: F4, and ●: P25). The chemical shifts measured at 295 K are plotted at time 0.

six TiO₂ photocatalysts are shown in Fig. 5. Chemical shifts are referred to DSS (sodium 2,2-dimethyl-2-silapentane-5-sulfonate) as an external reference. The values at time 0 indicate the chemical shifts measured at 295 K, which correspond to those of the mobile water molecules in layer III that are dominant before the temperature increase. Because the chemical shift differences among the six different photocatalysts at 295 K are small (within 0.5 ppm (6.2–5.7 ppm)), the chemical environments of the water molecules in the outermost layer (III) are considered to be similar among the six photocatalysts. When temperature is increased to 358 K, the longer the time after the temperature increase, the more diverse the chemical shift difference becomes. The chemical shifts of the broad water signals observed 2 h after the temperature increase correspond to the water molecules in layer I. For UV-100, AMT-600, and ST-01, the broad water signals appear in the lower field, whereas for F4, AMT-600, and P25, such signals appear in the higher field from those at 295 K. Thus, the fact that the chemical shifts and line widths of the water molecules near the solid surface are characteristic for the six photocatalysts with different properties indicates that the structure, mobility, and chemical environment of the water molecules in layer I are considerably diverse, reflecting the differences in the electronic and geometric structures of the underlying surface of individual photocatalysts.

The adsorbed water would be stabilized by various forces, in particular by hydrogen bonds, to form water associates. A hydrogen bond exerts a large influence on the ¹H NMR chemical shift and gives rise to a low-field shift of the resonance lines. As expected, the signals of adsorbed water molecules appear in the range from 6.5 to 5.4 ppm, which is lower than the location of liquid water (4.8 ppm at 295 K). Because the water molecules in layer I are considered to take more rigid structures that are stabilized by stronger hydrogen bonds than those in layers II and III, the water signals in layer I are expected to appear at lower field than those in layer III. However, as illustrated in Fig. 5, for the three photocatalysts (P25, F4, and AMT-600) the water signals in layer I appear in a higher field than those in layer III. This fact suggests the existence of more favorable factors that affect the chemical shifts other than hydrogen bonding.

Six different photocatalytic samples used in the present study were fabricated by the original preparation procedure developed by each supplier, which leads to the different crystal defect structures and surface morphologies. Surface defects and surface-adsorbed species affect significantly the electronic and geometric characteristics of TiO_2 surface and alter the chemical reactivity. Proton chemical shifts for the water molecules interacting with various types of surface sites must differ to some extent. The most important interacting sites would be surface hydroxyl groups. The interactions are mainly the formation of the hydrogen bond network between water molecules and surface hydroxyl groups. From the temperature dependence of IR spectra of the TiO_2 film of anatase, Finnie et al. reported that the terminally bound hydroxyl species observed at 3730 cm^{-1} are obscured by broadening and red shifting on H bonding with coordinated H_2O whereas it grows in intensity on the dehydration of the surface. In contrast, bridging hydroxyl species, which appear at 3670 cm^{-1} , do not undergo H-bonding interactions with H_2O . Above 373 K, the concentration of bridging hydroxyls is reduced by heating, but it is replenished by the dissociative absorption of H_2O on cooling to 398 K, when the molecular absorption of H_2O begins.⁴¹ As stated above, for the ^1H MAS NMR spectra of anatase TiO_2 samples the peaks, at 6.4 and 2.3 ppm were attributed to the positively charged acidic protons located on bridged O atoms, and to the basic H atoms bound to the terminal oxygen, respectively.³⁷ As illustrated in Fig. 6, the protons of water molecules in layer I undergoing chemical exchange with surface hydroxyl groups would shift to some extent, depending on the exchange rate and the amount of the surface hydroxyl groups. The high-field chemical shift of water signals in layer I observed for P25, F4, and AMT-600 might indicate the existence of the more-abundant basic H atoms bound to the terminal oxygen. Actually, one can find in Table 2 the correlation between the chemical shifts of water signals in layer I and the isoelectronic points measured for the individual photocatalysts, which are indicative of surface acidity.³⁸ The water peaks in layer I for TiO_2 with higher isoelectronic points incline to appear in the higher field. Thus, besides the hydrogen bonding, the acidity of the solid surface, which is intimately related to the photocatalytic activity, is apparently the major factor contributing to the observed chemical shift in layer I.

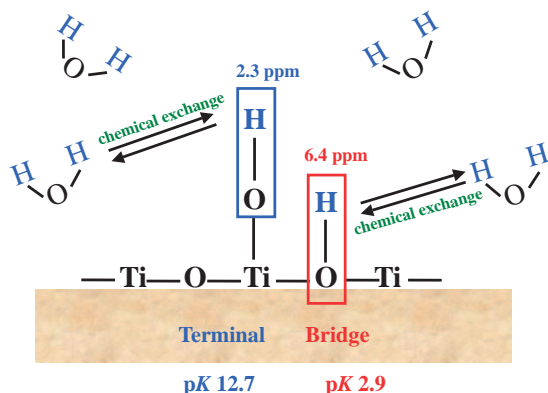


Fig. 6. Chemical shifts of ^1H NMR signals and pK values of surface OH of TiO_2 powders.

Table 2. The Chemical Shift of ^1H NMR Signals Measured at 358 K and Isoelectronic Points of TiO_2 Photocatalysts³⁸

TiO_2	Chemical shift ^{a)} /ppm	Isoelectronic point /pH
P25	5.4	4.1
F4	5.8	—
AMT-600	5.7	5.0
AMT-100	6.3	5.4
ST-01	6.1	5.9
UV-100	6.4	—

a) Chemical shift measured 4 h after temperature increase to 358 K.

Photocatalytic Reaction Site

TiO_2 photocatalytic degradation of a variety of environmentally hazardous organic compounds has been extensively investigated.^{1,2} Most investigations have been performed for the chemical species directly adsorbed on the surface after the evacuation of adsorbed water,^{31,81–87} assuming that the photoinduced reactions occur directly on the solid surface. However, it should be mentioned that in practical applications photocatalysts are utilized under aerobic conditions in the presence of adsorbed water, and photocatalysis can take place in adsorbed water regions. As stated above, the adsorbed water region consists of three water layers. Then, how are the organic pollutants incorporated into the photocatalytic systems in the presence of adsorbed water to be photo decomposed? In this section, we will discuss the adsorption and photodecomposition of pollutants in the presence of adsorbed water based on the experimental results observed by solid-state ^1H NMR spectroscopy.³⁴

Degussa P25 powder is used as TiO_2 photocatalyst and ethanol is employed as a model substrate of organic pollutants. As stated in the previous section, ^1H MAS NMR spectrum of P25 measured at the spinning rate of 12.6 kHz presents a single signal. Owing to this rapid rotation, when a small quantity of ethanol (170 nmol) is loaded onto the top of the NMR sample tube containing 25 mg of TiO_2 powder at 295 K, ethanol molecules rapidly diffuse in 30 min in the powder and give a small peak at 0.99 ppm with a line width of 750 Hz ascribed to methyl ($-\text{CH}_3$) protons of ethanol, as shown in Fig. 7. Methylene ($-\text{CH}_2$) and OH signals of ethanol are not observed due to the overlap with the adsorbed water signal of TiO_2 . With increasing temperature up to 358 K, the ethanol peak becomes sharper (line width, 240 Hz at 358 K), most probably due to the gained mobility, but the peak area and chemical shift barely change within the temperature range studied. Taking account of the chemical shift and the relatively sharp line width, one can attribute the peak to the ethanol molecules in the adsorbed water region but not to those directly adsorbed on the surface of metal oxide.

On the other hand, the adsorbed water peak shows similar temperature dependence to that in the absence of ethanol and the intensity becomes 40% of that at 295 K on keeping the temperature at 358 K for a long enough time (more than 2 h), as stated in the previous section. On reversion of the temperature to 295 K, ethanol presents still a peak with the same line width and intensity as that before the temperature in-

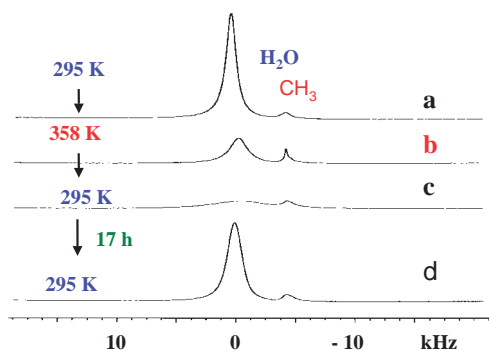


Fig. 7. ^1H MAS NMR spectra of TiO_2 powder (Degussa P25) on addition of ethanol of (170 nmol) measured at 500 MHz with spinning rate of 12.6 kHz at 295 K (a), 358 K (b), 295 K (c) (just after the temperature was decreased back to 295 K), and 295 K (d) (after the sample was kept at room temperature for 1 month).³⁴

crease, while the water peak is three times broader due to the evaporation of volatile water molecules in layers II and III. This means that the ethanol molecules incorporated in the photocatalytic system do not vaporize even at 358 K, but are firmly captured in the physisorbed water region, although a substantial amount of the adsorbed water molecules vaporize. The reduced water signal recovers almost completely in 20 h to present the same spectral feature as that before the temperature increase. On the other hand, ethanol keeps the same line shape even after 1 month (Fig. 7d).

In homogeneous liquid systems, ethanol molecules vaporize at lower temperature than water molecules. On the contrary, in this case physisorbed water molecules volatilize more easily than ethanol molecules, indicating that a small quantity of ethanol molecules are highly stabilized in the heterogeneous photocatalytic systems. This observation suggests that hydrogen bonding of ethanol with water molecules should be stronger than that among water molecules.

Then what happens when excess amounts of ethanol molecules are incorporated in the photocatalytic systems? Figure 8a shows the ^1H NMR spectrum of P25 powder saturated with ethanol molecules, which is packed in a 3-mm glass NMR sample tube and measured without magic angle spinning. In spite of the measurement without magic angle spinning, sharp and intensified water and the methylene ($-\text{CH}_2$, 3.67 ppm) and methyl ($-\text{CH}_3$, 1.0 ppm) signals of ethanol can be observed, indicating that ethanol molecules adsorb on the solid surface in fairly mobile states. The OH signal of ethanol overlaps with the water signal. When the sample is heated at 423 K for an hour, two very broad peaks are observed (Fig. 8b). As stated above, in the absence of ethanol the water peak disappears completely at 423 K. Therefore, these broad peaks could be ascribed to CH_2 and CH_3 originating from the ethanol molecule by taking account of the relative signal intensity of 2:3. On keeping this sample at room temperature under atmospheric conditions for more than several hours, with the recovery of the signal from physisorbed water that re-adsorbed on the surface of metal oxide from the air, relatively sharp ethanol signals gradually appear although the final intensity is reduced substantially. This signal remains unchanged in the photocatalytic system even after 1 month as shown in Fig. 8c. If one

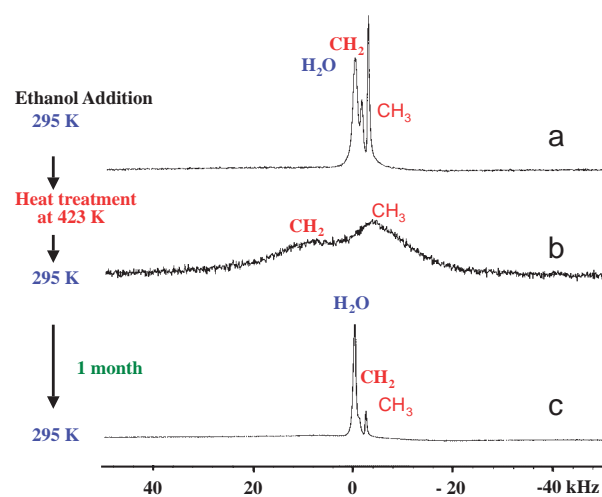


Fig. 8. ^1H NMR spectra of TiO_2 Degussa P25 with ethanol measured at 295 K. P25 was suspended in ethanol solution and vacuum-dried at room temperature. The sample was packed in a 3-mm glass tube and measured without rotation (a) before calcination, (b) after calcination at 423 K for 1 h in an electric furnace, and (c) after sample (b) was kept at room temperature for 1 month.³⁴

takes account of the sharp line width, one can conclude that ethanol molecules locate obviously in the physisorbed water regions in a mobile state. At 423 K physisorbed water molecules and most of the ethanol molecules vaporized. However, the ethanol molecules that reach the solid surface react with the surface titanols to form ethoxide, which gives rise to two resonance lines of OCH_2 and CH_3 with remarkable line broadening due to the restricted mobility. The amount of surface titanols is about 50 times smaller than that of physisorbed water.⁸⁸ Since the available amount of titanol is quite small, most of the ethanol molecules would vaporize. With the recovery of the water layers, the ethoxide would be hydrolyzed to form ethanol molecules that migrate back to the physisorbed water layer and give sharp NMR signals with reduced intensity. Thus, when large amounts of ethanol molecules are incorporated in the photocatalytic systems, a part of the ethanol molecules may interact with titanol on the solid surface to form ethoxide. In this case photo decomposition would take place directly on the solid surface. However, the present experimental facts imply that a small amount of ethanol would stay more preferably in the physisorbed water layers with high water content rather than near the solid surface region of the TiO_2 photocatalysts at room temperature in atmospheric conditions. After this sample is irradiated by UV for 1 h, only a water peak is observed, resulting from the complete decomposition of ethanol into H_2O and CO_2 .

The above observations are summarized in Fig. 9. At room temperature, the incorporated ethanol molecules are stabilized by the hydrogen bonds with water molecules in the physisorbed water layers, where both ethanol and water molecules are fairly mobile. On UV irradiation the ethanol molecules in this state are oxidized by the photogenerated active species to water and CO_2 . The concentration of the chemical species incorporated into the photocatalyst as a pollutant would be quite low. Industrial gas emissions often contain contaminants

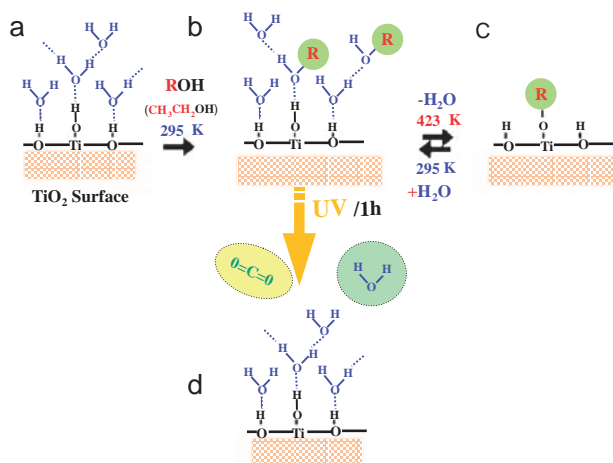


Fig. 9. Schematic illustration of the photocatalytic TiO₂ surface. (a) TiO₂ surface with water. (b) Ethanol molecules loaded preferably stay in the mobile physisorbed water layers. (c) On increasing temperature up to 423 K, water molecules in the inner phase would be replaced successively by ethanol and the ethanol molecules reaching the solid surface react with titanols to form ethoxide. At room temperature, the powder gradually readsorbs water molecules in the air and the ethoxide is hydrolyzed to ethanol, which returns to state (b). (d) Photocatalytic reactions of ethanol under atmospheric conditions take place in this state of the reactant, which decomposes to CO₂ and water via several intermediate species.³⁴

in low concentrations (<100 ppm) and flow at high rates, and under these conditions ethanol can be oxidized photocatalytically mainly in the mobile physisorbed water layers. Since the physisorbed water region consists of layers where water molecules take different structures and mobility, the mechanism of the interaction of ethanol with water molecules in each layer must be complicated.

The Adsorbed Water on TiO₂ Films

A number of photocatalytic studies have been concerned with TiO₂ powders due to the large specific surface area.¹⁴ However, the development of films with high photocatalytic activity has become important since the discovery of the intriguing properties of conversion between less hydrophilic and more hydrophilic character upon UV light irradiation. A surface coated with a transparent nanoparticulate TiO₂ film is originally less hydrophilic and water beads spread on the surface, resulting in fogging of a glass surface. However, after irradiation with UV light, the surface becomes highly hydrophilic, water wets the surface, and glass with an irradiated coating remains clear in a high humidity environment. The surface, however, gradually reverts to its originally less hydrophilic condition in the dark. The highly hydrophilic property opened new applications of TiO₂ coatings such as anti-fogging and self-cleaning. For example, TiO₂-coated side mirrors of automobiles would give a clear view even on a rainy day, and stains adsorbed on TiO₂-coated wall tiles can be easily washed off by rainwater.

Although some plausible mechanisms have been proposed for this phenomenon, it has not yet been completely under-

stood. It was reported that the high hydrophilicity of TiO₂ surfaces caused by UV irradiation arose from the dissociative adsorption of water on the photoinduced oxygen defects of TiO₂ surfaces to form surface hydroxyl groups.^{89–97} From the results of XPS, FT-IR, and the electrochemical experiments, the following mechanism has been proposed:⁹⁷ the photogenerated holes diffuse to the TiO₂ surface and are trapped at a lattice oxygen, which weakens the binding energy between the Ti and the lattice oxygen. A water molecule interrupts this bond to form new hydroxyl groups. In the dark, these hydroxyl groups gradually desorb from the surface in the form of H₂O₂ or H₂O + O₂. The hydroxyl groups produced by UV irradiation are thermodynamically less stable as compared to the hydroxyl groups bound to oxygen vacancies, which was suggested based on the results that the desorption temperature for the former is lower than that for the latter. Hence reconstruction from the stable hydroxyl groups to the thermodynamically metastable hydroxyl groups increases the surface energy of the TiO₂, leading to the hydrophilic conversion.⁹⁷ This mechanism may be supported by the experimental results that either the ultrasonic treatment or the wet rubbing treatment caused the removal of such OH groups, making the highly hydrophilic surface change to the less hydrophilic state immediately.^{89–96}

On the other hand, it has been demonstrated that the highly hydrophilic surface must be achieved by the degradation of adsorbed organic species on the surface through the oxidation process by the photogenerated holes.⁹⁸ Recently, White et al. demonstrated that TPD spectra of H₂O dosed on clean TiO₂ (110) surfaces exhibit wetting behavior either in the presence or the absence of surface oxygen vacancies and the associated surface-exposed Ti³⁺ cations. When covered with trimethyl acetate (TMA), water TPD spectra exhibit non-wetting behavior, but by irradiation with UV light in the presence of O₂, TMA is removed to restore the wetting behavior of the surface.⁹⁹ However, by taking account of the experimental results that sonication converts the photoproduct hydrophilic surface back to the original less hydrophilic surface within several minutes, and that strontium titanate (SrTiO₃), with almost the same photocatalytic oxidation power as TiO₂, exhibits no hydrophilic conversion on UV irradiation,⁹⁶ some other conversion mechanism seem to exist besides the degradation of adsorbed organic species on the surface. Although the mechanism is still controversial, in order to improve this prominent property and to develop new applications, the establishment of suitable and reliable methods for the quantitative evaluation of the hydrophilic conversion properties must be established.

Recently, we observed proton NMR signals of adsorbed water on TiO₂ film and found that the signals disappeared on UV irradiation in a closed system and recovered after the introduction of air but with a different spectral feature, possibly due to the photoinduced change of the TiO₂ surface environments.³³ In this review, we report recent ¹H NMR studies on water molecules adsorbed on TiO₂ film of anatase related to photoinduced surface conversion in an open system.³⁵

The TiO₂ film was prepared on SiO₂-coated soda-lime glass with a conventional Ar ion sputtering method employed for actual practical applications. The crystal structure of the film

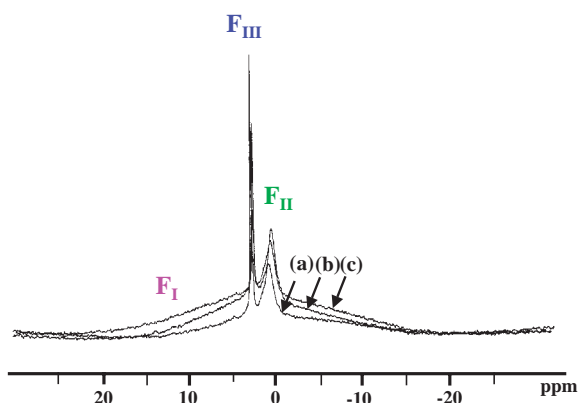


Fig. 10. ^1H NMR spectra measured at 800 MHz at 294 K: (a) an empty NMR sample tube, (b) substrate plates, and (c) TiO_2 film plates. Chemical shifts are referred to DSS as an external standard.

is anatase with the thickness of SiO_2 and TiO_2 layers of 64 and 180 nm, respectively. ^1H NMR observation of water signals adsorbed on TiO_2 thin film is rather difficult as compared to those for TiO_2 powders. The main problem arises from the much smaller quantity of water molecules which can be placed in a NMR sample tube in the form of thin films. In addition, the film sample can not be rotated with magic angle spinning. Due to the poor signal to noise ratio, the quantitative detection of ^1H NMR signals of adsorbed water on a single film plate placed in a NMR sample tube is seriously disturbed by proton signals arising from probe background, a glass NMR sample tube and a substrate glass plate. Therefore, one should be cautious about the interpretation of the spectra. The background signal of the NMR probe can be eliminated by subtracting the spectrum measured without a sample tube from the spectra of the sample. As shown in Fig. 10, the NMR glass sample tube (empty tube) presents water signals adsorbed on the glass materials. The spectrum consists of two sharp peaks (F_{III} and F_{II}) and one broad peak (F_{I}). On placing two substrate glass plates in the sample tube, a substantial increase in the signal intensities of peaks F_{I} and F_{II} is observed. When two TiO_2 film plates are placed in the sample tube, a further increase in intensities in peaks F_{I} and F_{II} is observed. Two plates are placed in a 5 mm o.d. glass sample tube so as to direct the TiO_2 -coated surface of the plates back to back.

Although distinctive discrimination of the water peaks among a NMR glass tube, substrates and TiO_2 films is difficult, Figure 10 obviously indicates that substantially larger amounts of water molecules are adsorbed on the TiO_2 film surface, which contribute to the enhancement of water signals F_{I} and F_{II} .

The line widths at a half-peak height of F_{I} – F_{III} are about 13 kHz, 600 Hz, and 120 Hz, respectively. These three NMR peaks indicate the presence of three distinct H_2O species. The spectral feature of TiO_2 thin film is clearly different from ^1H NMR spectra of TiO_2 powder, which present a single resonance line. As shown in Fig. 11, the sharpest peak F_{III} is readily suppressed by N_2 gas flow as compared to peaks F_{II} and F_{I} . Therefore, F_{III} corresponds to the most mobile water species located in the most outer phase of the photocatalysts, which exchanges slowly with gaseous water molecules in the space

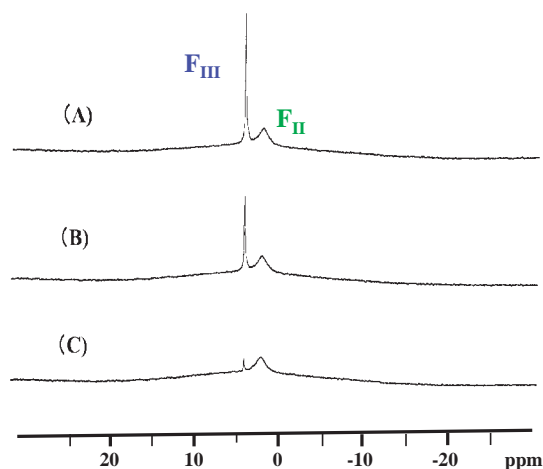


Fig. 11. ^1H NMR spectra measured at 800 MHz at 294 K (A) with a cap, and under N_2 flow (B) for 5 min, and (C) for 1 h. Chemical shifts are referred to DSS as an external standard.

of a NMR sample tube. Because powder samples are packed in the ZrO_2 sample tube without any vacant space in the sample tube and measured with contacting dry flowing air, F_{III} would be too small to be observed.

Provided that the line width is determined predominantly by the spin–spin relaxation rate of water proton, the mobility of the three different water species could be roughly estimated from the line widths. Taking into account the trend that the line width becomes sharper with an increase of mobility, we see that the molecular mobility of water would be higher in the order of $\text{F}_{\text{III}} > \text{F}_{\text{II}} > \text{F}_{\text{I}}$. The mobility of F_{III} would be roughly estimated to be several times larger than that of F_{II} and about two orders of magnitude larger than that of F_{I} . Peak F_{III} decreases in intensity upon becoming somewhat broader when substrate plates and TiO_2 film plates are placed in a sample tube. This phenomenon could be attributed to the change in magnetic inhomogeneity caused by placing the sample plates in the tube, because the sharpest signal is the most sensitive to the magnetic inhomogeneity. No further change is observed in the NMR probe without photoirradiation. The water species of F_{II} that are several times less mobile than those of F_{III} would be located in a rather inner position, and might correspond to water species in layers II and III for powder. The most immobile rigid water species of F_{I} would correspond to those near the TiO_2 solid surface. The obvious difference in the signal feature between F_{I} and the water species in layer I near the solid surface could be ascribed to the differences of the underlying surface structures. The surface of the thin film is more heterogeneous and must contain more defects or vacancies due to the preparation procedure of ion sputtering. This causes more diverse chemical environments of the water molecules near the solid surface resulting in a broad distribution of water signals with broad line widths like F_{I} .

For the IR measurements of a TiO_2 film of anatase under flowing dry air, Finnie et al. observed two types of coordinated H_2O species on the TiO_2 surface.⁴¹ The first species at 3696 and 3573 cm^{-1} (non-H-bonded and H-bonded, respectively) is relatively loosely held and is rapidly desorbed from the sur-

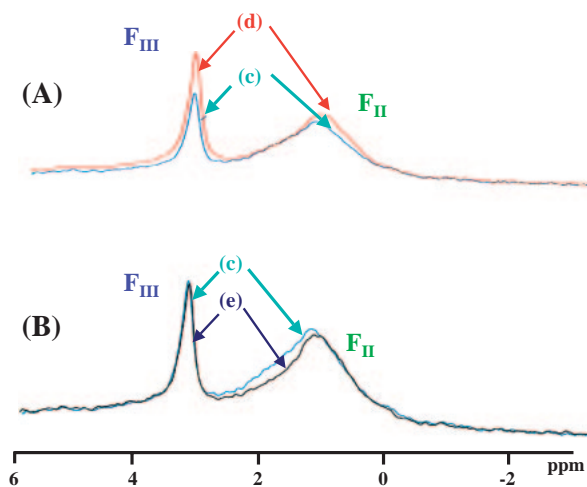


Fig. 12. ^1H NMR spectra of TiO_2 film plates measured at 800 MHz at 294 K: (A) (c) before and (d) just after 30 min UV irradiation in air; (B) (c) before (same as (c) in (A)) and (e) 2 h (stored in the dark) after 30 min UV irradiation in air.³⁵ Chemical shifts are referred to DSS as an external standard.

face with mild heating, which would correspond to FII. The second water species with bands at 3634 and 3474 cm^{-1} (non-H-bonded and H-bonded, respectively) is bound more strongly, and its concentration decreases slowly to below the detection limit with heating at 398 K, which is considered to correspond to FI.

As described above, a TiO_2 surface becomes highly hydrophilic on UV light irradiation and gradually reverts to the originally less hydrophilic state in the dark.^{89–97} The TiO_2 film prepared in the present study shows a water contact angle of 6.5° before UV irradiation. After 30 min UV irradiation, water droplets spread out on the film, resulting in a contact angle of 0°. And the contact angle reverts to 4.7° after the sample is kept in the dark for 2 h.

The hydrophilic conversions are quite well correlated with the changes of the NMR signal intensities. When the sample is UV irradiated outside the NMR probe in air (without a cap of the sample tube) for 30 min, a substantial amount of increase in the intensities of peaks FII and FIII is observed for TiO_2 film plates (Figs. 12A(d) and 13). From the difference spectrum between the spectra before and after UV irradiation (Fig. 13), although slight, an increase in the intensity in peak FI can also be observed. When the sample is kept in the dark for 2 h in air, the signal intensities of peaks FI–III revert to the initial state. Peak FIII reverts completely to the initial state in 2 h whereas peak FII presents a different signal shape and the signal intensity reduces slightly (Fig. 12B). Because the line shape of peak FII of the substrate plates is affected by UV irradiation for some reason (data are not shown), one can not conclude whether the signal change of peak FII after UV irradiation arises from the photoinduced effect on the substrate glass or from the chemical environmental change around the physisorbed water near the TiO_2 surface resulting from the photoinduced surface structural change.⁹⁷ However, for the substrate glass plates, on UV irradiation, peaks FI and FIII are not affected and no signal enhancement is observed for

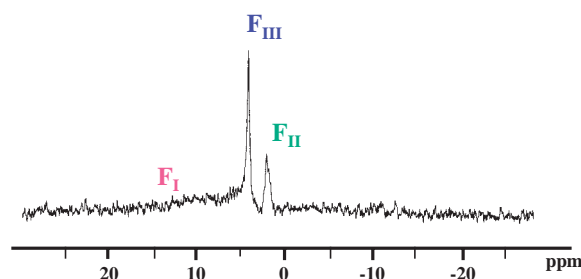


Fig. 13. Difference spectrum between the spectra before and just after 30 min UV irradiation measured at 800 MHz at 294 K (subtraction of (c) from (d) in Fig. 12A).³⁵

all the peaks. Therefore, this enhancement must be specific to the TiO_2 film. These results are highly reproducible.

In the previous studies for the TiO_2 film piece, changes of the spectral features of the water peak corresponding to peak FI were clearly detected before and after UV irradiation in a closed system, these could be ascribed to the photoinduced structural change.³³ In the present films, as shown in Fig. 13, the signal shapes of peak FI differ also before and after UV irradiation, reflecting the structural change of the solid surface, although the change is not so clearly detected as in the previous study because of the poor signal-to-noise ratio.

The characteristics of adsorbed water and surface hydroxyl groups have been extensively studied and related to the surface characteristics of TiO_2 by TPD and infrared reflection absorption spectroscopy (IRAS).^{16,21,24–32} The photoinduced hydrophilic surface of TiO_2 becomes less hydrophilic in an O_2 atmosphere in the dark. It was confirmed by XPS studies that, on UV irradiation in air, the total amount of the surface hydroxyl groups increased, but the amount of the surface hydroxyl groups bound to oxygen vacancy was found to decrease with TPD experiments.⁹⁷ Therefore, it was suggested that UV irradiation should increase the amount of water, which could not be observed in the TPD experiments.⁹⁷ Actually, the results of the TPD observation that started from the lower temperature indicated that a substantial amount of water molecules were desorbed from the TiO_2 surface below room temperature under vacuum.³² In addition, the photoadsorption of gaseous water on TiO_2 surfaces was also reported by surface-enhanced infrared absorption spectroscopy (SEIRAS).²⁹

The fact that the water photoadsorbed on TiO_2 was removed easily by O_2 suggested that the photoadsorption of water should be rather weak.

The increase of the molecularly adsorbed water on UV irradiation is clearly evidenced by NMR study that shows the enhancement of intensities of FIII.³⁵ The fact that the chemical shift of FIII is unchanged before and after UV irradiation evidently indicates that the adsorption of this water occurs molecularly but not dissociatively. Three kinds of water species represented by FI–FIII might exchange among three different states slowly on the NMR time scale. The strong interaction among different kinds of hydroxyl groups is also indicated by SEIRAS measurements.²⁹ Several plausible factors responsible for the photoinduced hydrophilicity on TiO_2 films have been proposed as stated above.^{89–97} Although the photoinduced structural change on the TiO_2 surface has not been completely

elucidated, it must be one of the most important factors. The photoinduced change of the TiO₂ surface environments (structures) would cause the change of the binding states of the surface hydroxyl groups and/or the change of the structures of water associates in the inner layer near the solid surface, resulting in the enhancement of the hydrophilicity. This change would lead to the successive enhancement of the water contents of the intermediate and the outer layers, resulting in the observed large enhancement of NMR peaks FIII and FII, because water molecules are considered to exchange slowly among the three water states.

Conclusion

The investigation of properties of water molecules adsorbed on anatase-abundant TiO₂ in powder and film forms by ¹H NMR spectroscopy revealed that the physisorbed water region is categorized by four distinctively different states, comprising i) rigid water species with restricted mobility near the solid surface, ii) less mobile water molecules in the intermediate water layer, iii) relatively mobile water molecules in the outer water layer, iv) very loosely adsorbed water molecules which exchange slowly with gaseous water molecules in air. The thickness of the water layers i)–iii) for anatase-abundant TiO₂ powders is found to be almost the same, although they possess different physical properties such as primary particle size, crystal size, crystal form, and BET surface area. For powder, the number of water molecules contained in states i), ii), and iii) could be roughly estimated to be 4.8×10^{14} , 3.2×10^{14} , and 8.0×10^{14} molecules/cm². The water molecules in the innermost layer are quite sensitively influenced by the surface environment of the individual photocatalysts.

It has been demonstrated that ethanol molecules in practical conditions as contaminants are firmly captured in mobile physisorbed water layers to be photodecomposed to CO₂ and water after photoillumination. This fact suggests that the actual photocatalytic oxidation of organic compounds of low concentration, along with that for most of the environmental pollutants, can be favored in the physisorbed water region rather than on the solid surface.

The conversion of wettability induced by photo irradiation is well reflected in the NMR signal change. The enhancement of the signal intensity of water molecularly adsorbed on TiO₂ films could be observed on UV irradiation by ¹H NMR spectroscopy; such enhancement has been difficult to elucidate so far with alternative spectroscopic techniques.

Thus, ¹H NMR spectroscopy could provide novel as well as complementary information on the characteristics of adsorbed water and adsorbed species, although it has not been extensively applied to photocatalytic systems so far.

This work was performed under the Cooperative Research Program of the Institute for Protein Research, Osaka University, and financially supported in part by a Grant-in-Aid on the Priority Area (417) from the Ministry of Education, Culture, Sports, Science and Technology (MEXT) and also by the Core Research for Evolution Science and Technology (CREST) from the Japan Science and Technology Agency (JST). The authors are grateful to Mr. E. Kojima, and Drs. H. Akutsu, T. Fujiwara, H. Yagi, and T. Ikegami, for their cooperation.

References

- 1 M. R. Hoffmann, S. T. Martin, W. Choi, and D. W. Bahnemann, *Chem. Rev.*, **95**, 69 (1995).
- 2 A. Fujishima, T. N. Rao, and D. A. Tryk, *J. Photochem. Photobiol., C*, **1**, 1 (2000).
- 3 K. Honda and A. Fujishima, *Nature*, **238**, 37 (1972).
- 4 M. A. Fox and M. T. Dulay, *Chem. Rev.*, **93**, 341 (1993).
- 5 M. Grätzel, "Energy Resources through Photochemistry and Catalysis," Academic Press (1983).
- 6 "Photocatalysis: Fundamentals and Applications," ed by N. Serpone and E. Pelizzetti, Wiley, New York (1989).
- 7 "Photocatalytic Purification and Treatment of Water and Air," ed by D. F. Ollis and H. Al-Ekabi, Elsevier (1993), p. 820.
- 8 "Heterogeneous Photocatalysis," ed by M. Schiavello, John Wiley, Chichester (1997), p. 197.
- 9 A. Fujishima, K. Hashimoto, and T. Watanabe, "TiO₂ Photocatalysis: Fundamentals and Applications," BKC, Tokyo (1999).
- 10 "Photocatalysis," ed by M. Kaneko and I. Ohkura, Kodansha-Springer, Tokyo (2002).
- 11 Y. Nosaka, S. Komori, K. Yawata, T. Hirakawa, and A. Y. Nosaka, *Phys. Chem. Chem. Phys.*, **5**, 4731 (2003).
- 12 A. Kudo, *Catal. Surv. Asia*, **7**, 31 (2003).
- 13 M. Anpo, *Bull. Chem. Soc. Jpn.*, **77**, 1427 (2004).
- 14 G. D. Parfitt, *Prog. Surf. Membr. Sci.*, **11**, 181 (1976).
- 15 S. Sato, T. Kadowaki, and K. Yamaguti, *J. Phys. Chem.*, **88**, 2930 (1984).
- 16 S. Sato, *J. Phys. Chem.*, **91**, 2895 (1987).
- 17 A. Lopez, M. H. Tuillier, J. L. Guth, L. Delmotte, and J. M. Popa, *J. Solid State Chem.*, **102**, 480 (1993).
- 18 J. Blanchard, C. Bonhomme, J. Maquet, and C. J. Sanchez, *Mater. Chem.*, **8**, 985 (1998).
- 19 M. B. Hugen Schmidt, L. Gamble, and C. T. Campbell, *Surf. Sci.*, **302**, 329 (1994).
- 20 H. P. Boehm, *Discuss. Faraday Soc.*, **52**, 264 (1971).
- 21 G. Munuera and F. S. Stone, *Discuss. Faraday Soc.*, **52**, 205 (1971).
- 22 M. A. Henderson, *Surf. Sci.*, **355**, 151 (1996).
- 23 M. A. Henderson, *Langmuir*, **12**, 5093 (1996).
- 24 P. Jones and J. A. Hockey, *Trans. Faraday Soc.*, **67**, 2669 (1971).
- 25 P. Jones and J. A. Hockey, *Trans. Faraday Soc.*, **67**, 2679 (1971).
- 26 M. Primet, P. Pichat, and M. V. Mathieu, *J. Phys. Chem.*, **75**, 1216 (1971).
- 27 D. D. Beck, J. M. White, and C. T. Ratcliffe, *J. Phys. Chem.*, **90**, 3123 (1986).
- 28 L. A. Phillips and G. B. Raupp, *J. Mol. Catal.*, **77**, 297 (1992).
- 29 R. Nakamura, K. Ueda, and S. Sato, *Langmuir*, **17**, 2298 (2001).
- 30 L. Shao, L. Zhang, M. Chen, H. Lu, and M. Zhou, *Chem. Phys. Lett.*, **343**, 178 (2001).
- 31 S. H. Szczepankiewicz, A. J. Colussi, and M. R. Hoffmann, *J. Phys. Chem. B*, **104**, 9842 (2000).
- 32 M. A. Henderson, *Surf. Sci. Rep.*, **464**, 1 (2002).
- 33 A. Y. Nosaka, T. Fujiwara, H. Yagi, H. Akutsu, and Y. Nosaka, *Chem. Lett.*, **2002**, 420.
- 34 A. Y. Nosaka, T. Fujiwara, H. Yagi, H. Akutsu, and Y. Nosaka, *Langmuir*, **19**, 1935 (2003).
- 35 A. Y. Nosaka, E. Kojima, T. Fujiwara, H. Yagi, H. Akutsu,

and Y. Nosaka, *J. Phys. Chem. B*, **107**, 12042 (2003).

36 A. Y. Nosaka, T. Fujiwara, H. Yagi, H. Akutsu, and Y. Nosaka, *J. Phys. Chem. B*, **108**, 9121 (2004).

37 V. M. Mastikhin, I. L. Mudrakovsky, and A. V. Nosov, *Prog. Nucl. Magn. Reson. Spectrosc.*, **23**, 259 (1991).

38 Y. Teraoka, Y. Shibata, and H. Kusaba, Proceeding of 24th Reference Catalysts Meeting, Catalysis Society of Japan (2003), p. 24.

39 P. A. Theil and T. E. Madey, *Surf. Sci. Rep.*, **7**, 211 (1987).

40 Y. Suda and T. Morimoto, *Langmuir*, **3**, 786 (1987).

41 K. S. Finnie, D. J. Cassidy, J. R. Bartlett, and J. L. Woolfrey, *Langmuir*, **17**, 816 (2001).

42 H. P. Boehm, *Adv. Catal.*, **16**, 179 (1966).

43 H. Knozinger, *Adv. Catal.*, **25**, 184 (1976).

44 M. Primet, P. Pichat, and M. V. Mathieu, *J. Phys. Chem.*, **75**, 1221 (1971).

45 D. J. C. Yates, *J. Phys. Chem.*, **65**, 746 (1961).

46 P. A. Cox, R. G. Egdel, and P. D. Naylor, *J. Electron Spectrosc. Relat. Phenom.*, **29**, 247 (1983).

47 R. G. Egdel and P. D. Naylor, *Chem. Phys. Lett.*, **91**, 200 (1982).

48 W. S. Epling, C. H. F. Peden, M. A. Henderson, and U. Diebold, *Surf. Sci.*, **412**, 333 (1998).

49 M. A. Henderson, *Mater. Res. Soc. Symp. Proc.*, **357**, 91 (1995).

50 M. A. Henderson, *Surf. Sci.*, **400**, 203 (1998).

51 G. Thornton, *Springer Ser. Surf. Sci.*, **33**, 115 (1993).

52 V. E. Henrich, *Springer Ser. Surf. Sci.*, **33**, 125 (1993).

53 R. L. Kurz and V. E. Henrich, *Phys. Rev. B*, **26**, 6682 (1982).

54 K. E. Smith and V. E. Henrich, *Phys. Rev. B*, **32**, 5384 (1982).

55 S. Suzuki, K. I. Fukui, H. Onishi, T. Sasaki, and Y. Iwasawa, *Stud. Surf. Sci. Catal.*, **132**, 753 (2001).

56 J. Fraissard, I. Solomon, R. Caillat, J. Elston, and B. Imelik, *J. Chim. Phys.*, **1963**, 676.

57 J. Kermarec, J. Fraissard, and B. Imelik, *J. Chim. Phys.*, **1968**, 920.

58 D. Freude, D. Müller, and H. Schmiedel, *Surf. Sci.*, **25**, 289 (1971).

59 R. L. Stevenson, *J. Catal.*, **21**, 113 (1971).

60 J. Demarquay, J. Fraissard, and B. Imelik, *C. R. Acad. Sci., Ser. C*, **273**, 1405 (1971).

61 V. Ladizhansky, G. Hodes, and S. Vega, *J. Phys. Chem. B*, **104**, 1939 (2000).

62 T. Ueda and N. Nakamura, *J. Phys. Chem. B*, **107**, 1368 (2003).

63 M. A. Enriquez, C. Doremieux-Morin, and J. Fraissard, *Appl. Surf. Sci.*, **5**, 180 (1980).

64 M. A. Enriquez, C. Doremieux-Morin, and J. Fraissard, *J. Solid State Chem.*, **40**, 233 (1981).

65 V. L. Zarcko and G. M. Kozub, *Ukr. Khim. Zh.*, **59**, 704 (1993).

66 V. I. Bogillo, V. V. Turov, and A. Vöelkel, *J. Adhes. Sci. Technol.*, **11**, 1513 (1997).

67 V. I. Bogillo, V. V. Turov, and A. Vöelkel, *J. Adhes. Sci. Technol.*, **11**, 1532 (1997).

68 D. E. Wöessner, *J. Magn. Reson.*, **39**, 297 (1979).

69 H. Pfeifer, *Nucl. Magn. Reson.*, **7**, 53 (1972).

70 K. J. Packer, *Prog. Nucl. Magn. Reson. Spectrosc.*, **3**, 87 (1967).

71 H. A. Resing, *Adv. Mol. Relax. Processes.*, **1**, 109 (1968).

72 A. Abragam, "The Principles of Nuclear Magnetism," Oxford University Press, Oxford (1961).

73 C. P. Slichter, "Principles of Magnetic Resonance," Third England and Updated Edition, Springer (1990).

74 K. Wüthrich, "NMR of Proteins and Nucleic Acids," Academic Press (1987).

75 J. Cavanagh, W. J. Fairbrother, A. G. Palmer, III, and N. J. Skelton, "Protein NMR Spectroscopy: Principles and Practice," Academic Press (1996).

76 F. J. M. van de Ven, "Multidimensional NMR in Liquids: Basic Principles and Experimental Methods," Wiley-VCH (1995).

77 J. Tabony, *Prog. Nucl. Magn. Reson. Spectrosc.*, **14**, 1 (1980).

78 "Water and Aqueous Solution at Subzero Temperatures," in "Water: A Comprehensive Treatise," ed by F. Franks, Plenum Press, New York (1982), Vol. 7.

79 V. V. Turov, E. A. Bakai, A. V. Turov, V. N. Barvinchenko, and M. Y. Kornilov, *Biofizika*, **35**, 765 (1990).

80 Y. Nosaka, M. Kishimoto, and J. Nishino, *J. Phys. Chem. B*, **102**, 10279 (1998).

81 I. Carrizosa and G. Munuera, *J. Catal.*, **49**, 174 (1977).

82 I. Carrizosa and G. Munuera, *J. Catal.*, **49**, 189 (1977).

83 K. S. Kim, M. A. Barteau, and W. E. Farneth, *Langmuir*, **4**, 533 (1988).

84 V. S. Lusvardi, M. A. Barteau, and W. E. Farneth, *J. Catal.*, **153**, 41 (1995).

85 M. R. Nimlos, E. J. Wolfrum, M. L. Brewer, J. A. Fennell, and G. Binter, *Environ. Sci. Technol.*, **30**, 3102 (1996).

86 S. J. Hwang, C. Petucci, and D. Raftery, *J. Am. Chem. Soc.*, **120**, 4388 (1998).

87 S. J. Hwang and D. Raftery, *Catal. Today*, **49**, 353 (1999).

88 T. Hirakawa, Y. Nakaoka, J. Nishino, and Y. Nosaka, *J. Phys. Chem. B*, **103**, 4399 (1999).

89 R. Wang, K. Hashimoto, A. Fujishima, M. Chikuni, E. Kojima, A. Kitamura, M. Shimohigoshi, and T. Watanabe, *Nature*, **388**, 431 (1997).

90 R. Wang, K. Hashimoto, A. Fujishima, M. Chikuni, E. Kojima, A. Kitamura, M. Shimohigoshi, and T. Watanabe, *Adv. Mater.*, **10**, 135 (1998).

91 N. Sakai, R. Wang, A. Fujishima, T. Watanabe, and K. Hashimoto, *Langmuir*, **14**, 5918 (1998).

92 T. Watanabe, A. Nakajima, R. Wang, M. Minabe, S. Koizumi, A. Fujishima, and K. Hashimoto, *Thin Solid Films*, **351**, 260 (1999).

93 R. Wang, N. Sakai, S. Koizumi, A. Fujishima, T. Watanabe, and K. Hashimoto, *J. Phys. Chem. B*, **103**, 2188 (1999).

94 M. Miyauchi, A. Nakajima, K. Hashimoto, A. Fujishima, K. Hashimoto, and T. Watanabe, *Chem. Mater.*, **12**, 3 (2000).

95 M. Miyauchi, A. Nakajima, K. Hashimoto, and T. Watanabe, *Adv. Mater.*, **12**, 1923 (2000).

96 N. Sakai, A. Fujishima, T. Watanabe, and K. Hashimoto, *J. Phys. Chem. B*, **105**, 3023 (2001).

97 N. Sakai, A. Fujishima, T. Watanabe, and K. Hashimoto, *J. Phys. Chem. B*, **107**, 1028 (2003).

98 C. Wang, H. Gröezin, and M. J. Shultz, *Langmuir*, **19**, 7330 (2003).

99 J. M. White, J. Szanyi, and M. A. Henderson, *J. Phys. Chem. B*, **107**, 9029 (2003).



Atsuko Y. Nosaka completed her Ph.D. from the Graduate School of Science of Kyoto University in 1977. She was a Post doctoral research fellow of Alexander von Humboldt Foundation at Max-Planck-Institute in Heidelberg (1978–1979), a research associate at The University of Texas Austin (1985–1986) a senior research associate at GRI-NIH, Baltimore, (1986–1987), a research associate of Tokushima University (1987–1989), and a research group leader at the International Research Laboratory of Ciba-Geigy AG (1989–98). She is presently a researcher of a project conducted by the New Energy and Industrial Technology Development Organization (NEDO). Her main research areas are (1) characterization of water molecules adsorbed on solid and membrane surfaces and (2) structural characterization of biomolecules mainly by means of NMR spectroscopy.



Yoshio Nosaka finished his doctoral course in Chemistry of Graduate School of Science, Kyoto University in 1977 with Prof. K. Akasaka and became an Encouraged Researcher of JSPS (Kyoto University), a Fellow at the RIKEN Institute, Wako (1978–1980 with Drs. A. Kira and M. Imamura) and joined the faculty of the Nagaoka University of Technology (1980–present). He was away from the university as a visiting researcher at The University of Texas, Austin (1985–1986, with Prof. M. A. Fox). His main research areas are physical chemistry of advanced materials, especially the reaction mechanism of TiO_2 photocatalysts, photoelectrochemistry of semiconductors, and chemical solution method of semiconductor nanoparticles.